Z. Angew. Math. Phys. (2020) 71:160

0044-2275/20/050001-15
published online September 3, 2020
https://doi.org/10.1007/s00033-020-01390-w

Zeitschrift für angewandte Mathematik und Physik ZAMP

Perturbed rigid body motions of an elastic rectangle

Julius Kaplunov and Onur Şahin

Abstract. Plane and anti-plane dynamic problems for an elastic rectangle loaded along its sides are considered. Low-frequency perturbations to rigid body translations are calculated. The derivation involves the solutions of non-homogeneous boundary value problems for harmonic and bi-harmonic equations. The explicit solution for the harmonic problem for transverse anti-plane translation is expressed through Fourier series. The bi-harmonic problem corresponding to the longitudinal in-plane translation is studied in greater detail for an elongated rectangle, which also may be treated using the elementary theory for plate extension. The derived perturbations incorporate the variations of displacements and stresses over the interior of the rectangle, including the case of self-equilibrated loading. The latter is obviously outside the range of validity of the classical rigid body framework.

Mathematics Subject Classification. 74B05, 74H45, 74G10.

Keywords. Low-frequency, Perturbation, Rigid body motion, Elastic rectangle.

1. Introduction

Newton's second law for a material point is also valid for calculating the accelerations at each point of a solid of a finite size provided the solid performs a rigid body motion, i.e. its deformation is negligible, e.g. [1]. This assumption usually appears to be pretty natural at sufficiently low vibration frequencies but inevitably fails at higher frequencies when internal structure and related resonance phenomena have to be taken into consideration. In the latter case, Newton's law can be generalized by introducing a frequency-dependent anisotropic mass density [2]. The concept of a negative mass appears to be fruitful for theoretical and experimental investigations of metamaterials, e.g. see [3–7].

At the same time, even over a low-frequency range well below a resonance domain, corrections to rigid body dynamics seem to be of interest. The point is that the classical set-up excludes the possibility of incorporating the effects of self-equilibrated loading, internal dissipation, inhomogeneity and deformability. Evaluation of all of them is inspired by modern engineering applications, including railway transport. In particular, the role of self-equilibrated longitudinal forces may be essential for modelling of high-speed impacts of freight cars, especially those subject to substantial compression, e.g. see [8–10].

Low-frequency perturbations to rigid body rotation and translations are deduced in [11] for dimensional bending and extension of an inhomogeneous viscoelastic bar. For a general linear viscoelastic kernel, the sought for corrections to the convention equations in rigid body dynamics is expressed through integral-differential operators acting on prescribed end longitudinal and transverse forces and bending moments. The derived equations allow calculating the variations of displacements along the bar subject to self-equilibrated loading.

We also mention the papers [11–15] considering almost rigid body motions of stiff components in strongly inhomogeneous elastic bars. In addition, the deviations from rigid body motions may be relevant for modelling of robotic and impact systems, e.g. see [16–18].

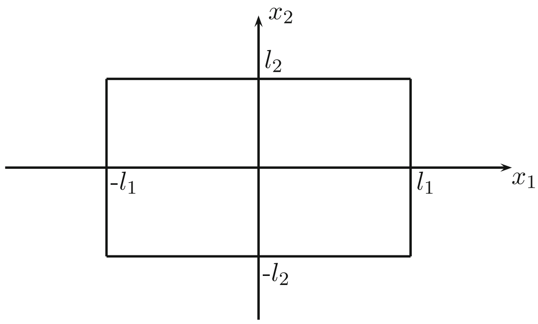

FIG. 1. An elastic rectangle

In this paper, we extend the one-dimensional analysis in [11] to two-dimensional plane and anti-plane problems for an elastic rectangle subject to given stresses along its sides. A typical time scale is assumed to be much greater than the time elastic waves travel the distance between the opposite sides of the rectangle. The stresses and displacements are expanded in asymptotic series expressed through the associated small parameter. As might be expected, the leading order terms in these expansions correspond to rigid body motions. The first-order corrections to rigid body motions come from the solutions of in-homogeneous pseudo-static problems (without inertial terms in the partial differential equations in linear elasticity). Such anti-plane problem has a simple explicit solution in terms of Fourier series as well as the original time-harmonic problem. Comparison of the exact and asymptotic solutions is presented in the paper for prescribed stresses of a parabolic variation. At the same time for the plane problem, the correction in question takes an easy to use the form only for an elongate rectangle, for which the related one-dimensional plate equations are valid. In the general case, the aforementioned pseudo-static problem may be easily reduced to a famous bi-harmonic problem, e.g. see [19–21] and references therein. The presentation is split into two sections corresponding to anti-plane and plane problems. Each of the sections contains the statement of the studied problem along with its asymptotic solution. The section for the anti-plane problem also involves a numerical example, whereas one of the focuses of the section concerned with the plane problem is on an elongated rectangle.

2. Anti-plane problem

Consider the anti-plane dynamic problem in linear elasticity for an elastic rectangle $\{(x_1, x_2) : |x_1| \leq l_1, |x_2| \leq l_2\}$ subject to edge loads, see Fig. 1.

The equation of motion for anti-plane motion of the rectangle may be written as

$$\sigma_{i3,i} = \rho u_{3,tt} \tag{1}$$

where u_3 is out of plane displacement and σ_{i3} are stress tensor components, t is time and ρ is mass density; also the summation convention is applied over the suffix $i = 1, 2$. The boundary conditions are given by

$$\sigma_{13}(\pm l_1, x_2, t) = P^{\pm}, \quad \sigma_{23}(x_1, \pm l_2, t) = Q^{\pm}, \tag{2}$$

where $P^{\pm} = P^{\pm}(x_2, t)$ and $P^{\pm} = Q^{\pm}(x_1, t)$ are prescribed loads. The stress components are expressed through the displacements as

$$\sigma_{i3} = \frac{E}{2(1+\nu)} \frac{\partial u_3}{\partial x_i}, \quad i = 1, 2, \tag{3}$$

where E is Young's modulus and ν is Poisson's ratio.

In this section, we consider the low-frequency motions of the rectangle perturbing its rigid body motion for which $u_3 = const$ and $\sigma_{i3} = 0$. To this end, we specify a small parameter related to the low-frequency regime as

$$\lambda = \frac{l_1}{Tc_2} \ll 1, \tag{4}$$

where T is a typical time scale and $c_2 = \sqrt{E/2\rho(1+\nu)}$; for harmonic vibrations with angular frequency ω, $T = 2\pi/\omega$ and $\lambda = \omega l_1/2\pi c_2 \ll 1$.

2.1. Perturbation procedure

First, we introduce dimensionless variables

$$y_i = \frac{x_i}{l_i}, \quad \tau = \frac{t}{T} \tag{5}$$

and dimensionless quantities

$$\sigma_{i3}^* = \frac{\sigma_{i3}}{\lambda^2 \rho\, c_2^2}, \quad u_3^* = \frac{u_3}{l_1}, \quad P_*^{\pm} = \frac{P^{\pm}}{\lambda^2 \rho\, c_2^2}, \quad Q_*^{\pm} = \frac{Q^{\pm}}{\lambda^2 \rho\, c_2^2}. \tag{6}$$

Then, the formulae above become

$$\sigma_{13,1}^* + \delta \sigma_{23,2}^* = u_{3,\tau\tau}^* \tag{7}$$

and

$$\begin{aligned} \lambda^2 \sigma_{13}^* &= \frac{\partial u_3^*}{\partial y_1}, \\ \lambda^2 \sigma_{23}^* &= \delta \frac{\partial u_3^*}{\partial y_2} \end{aligned} \tag{8}$$

with

$$\sigma_{13}^*\big|_{y_1=\pm 1} = P_*^{\pm}, \quad \sigma_{23}^*\big|_{y_2=\pm 1} = Q_*^{\pm} \tag{9}$$

where $\delta = l_1/l_2$.

Let us now expand the displacement and stress components into asymptotic series as

$$\begin{aligned} u_3^* &= u_3^{(0)} + \lambda^2 u_3^{(1)} + \cdots, \\ \sigma_{i3}^* &= \sigma_{i3}^{(0)} + \lambda^2 \sigma_{i3}^{(1)} + \cdots, \quad i = 1, 2. \end{aligned} \tag{10}$$

On substituting asymptotic expansions (10) into equation of motion (7), Eq. (8) and boundary conditions (9), we arrive at leading order boundary value problem

$$\sigma_{13,1}^{(0)} + \delta \sigma_{23,2}^{(0)} = u_{3,\tau\tau}^{(0)} \tag{11}$$

with

$$\sigma_{13}^{(0)}\big|_{y_1=\pm 1} = P_*^{\pm}, \quad \sigma_{23}^{(0)}\big|_{y_2=\pm 1} = Q_*^{\pm} \tag{12}$$

and

$$\frac{\partial u_3^{(0)}}{\partial y_1} = 0, \quad \frac{\partial u_3^{(0)}}{\partial y_2} = 0. \tag{13}$$

It is clear from Eq. (13) that

$$u_3^{(0)} = U(\tau), \tag{14}$$

which is the only leading order rigid body motion for the studied anti-plane problem. Next, we integrate (11) over the rectangular region taking into account (12) and (14). The result is

$$\begin{aligned}
&\int_{-1}^{1}\int_{-1}^{1} \frac{\partial \sigma_{13}^{(0)}}{\partial y_1} \mathrm{d}y_1 \mathrm{d}y_2 + \delta \int_{-1}^{1}\int_{-1}^{1} \frac{\partial \sigma_{23}^{(0)}}{\partial y_2} \mathrm{d}y_2 \mathrm{d}y_1 \\
&= \int_{-1}^{1} \left(\sigma_{13}^{(0)}\Big|_{y_1=1} - \sigma_{13}^{(0)}\Big|_{y_1=-1} \right) \mathrm{d}y_2 + \delta \int_{-1}^{1} \left(\sigma_{23}^{(0)}\Big|_{y_2=1} - \sigma_{23}^{(0)}\Big|_{y_2=-1} \right) \mathrm{d}y_1 \\
&= \int_{-1}^{1} \left(P_*^+ - P_*^-\right) \mathrm{d}y_2 + \delta \int_{-1}^{1} \left(Q_*^+ - Q_*^-\right) \mathrm{d}y_1 = 4U_{\tau\tau}.
\end{aligned} \tag{15}$$

At the leading order

$$u_{3,\tau\tau}^{(0)} = \frac{1}{4} \left(\int_{-1}^{1} \left(P_*^+ - P_*^-\right) \mathrm{d}y_2 + \delta \int_{-1}^{1} \left(Q_*^+ - Q_*^-\right) \mathrm{d}y_1 \right), \tag{16}$$

which corresponds, as expected, to Newton's second law

$$m\, u_{3,tt} = \frac{1}{4} \left(\int_{-l_2}^{l_2} \left(P^+ - P^-\right) \mathrm{d}x_2 + \delta \int_{-l_1}^{l_1} \left(Q^+ - Q^-\right) \mathrm{d}x_1 \right), \tag{17}$$

where $m = l_1\, l_2\, \rho$.

At next order, Eqs. (7)–(9) take the form non-homogeneous harmonic problem given by

$$\frac{\partial^2 u_3^{(1)}}{\partial y_1^2} + \delta^2 \frac{\partial^2 u_3^{(1)}}{\partial y_2^2} = u_{3,\tau\tau}^{(0)} \tag{18}$$

with

$$\left.\frac{\partial u_3^{(1)}}{\partial y_1}\right|_{y_1=\pm 1} = P_*^\pm, \qquad \delta \left.\frac{\partial u_3^{(1)}}{\partial y_2}\right|_{y_2=\pm 1} = Q_*^\pm. \tag{19}$$

For the sake of simplicity, we now assume that $P_*^\pm$ are even in y_2 and $Q_*^\pm = 0$. In this case, the solution, $u_{3c}^{(1)}$, of homogeneous equation (18) subject to boundary conditions (19) is

$$u_{3c}^{(1)}(y_1, y_2, \tau) = \sum_{n=1}^{\infty} \left(A_n \cosh \beta_n\, \delta\, y_1 + B_n \sinh \beta_n\, \delta\, y_1\right) \cos \beta_n\, y_2, \tag{20}$$

with $\beta_n = n\pi$ and the coefficients A_n and B_n given by

$$A_n = \frac{1}{2\beta_n \delta \sinh \beta_n \delta} \int_{-1}^{1} \left(P_*^+ - P_*^-\right) \cos \beta_n y_2 \mathrm{d}y_2 \tag{21}$$

and

$$B_n = \frac{1}{2\beta_n \delta \cosh \beta_n \delta} \int_{-1}^{1} \left(P_*^+ + P_*^-\right) \cos \beta_n y_2 \mathrm{d}y_2. \tag{22}$$

On the other hand, the particular solution of equation (18) subject to homogeneous boundary conditions (19) may be written as

$$u_{3p}^{(1)} = a_1 y_1^2 + a_2 y_1 + a_3. \tag{23}$$

On substituting it into (18) we have

$$a_1 = \frac{1}{8} \int_{-1}^{1} \left(P_*^+ - P_*^-\right) \mathrm{d}y_2. \tag{24}$$

Solution (23) should also satisfy boundary condition (12), yielding

$$a_2 = \frac{1}{4} \int_{-1}^{1} \left(P_*^+ + P_*^-\right) \mathrm{d}y_2 \tag{25}$$

In order to find coefficient a_3, we proceed to a higher order, having from the formulae above

$$\sigma_{13,1}^{(1)} + \delta \sigma_{23,2}^{(1)} = u_{3,\tau\tau}^{(1)} \tag{26}$$

and

$$\sigma_{13}^{(1)}\big|_{y_1=\pm 1} = \sigma_{23}^{(1)}\big|_{y_2=\pm 1} = 0 \tag{27}$$

along with

$$\sigma_{13}^{(0)}\big|_{y_1=\pm 1} = P_*^{\pm} \tag{28}$$

where $u_3^{(1)} = u_{3c}^{(1)} + u_{3p}^{(1)}$. Integrating (26) over the rectangular area and applying boundary conditions (27), we get

$$\int_{-1}^{1} \int_{-1}^{1} u_{3c}^{(1)} \mathrm{d}y_1 \mathrm{d}y_2 + 2 \int_{-1}^{1} u_{3p}^{(1)} \mathrm{d}y_1 = 0. \tag{29}$$

It readily follows from (20) that the repeated integral in (29) vanishes. Then

$$a_3 = -\frac{1}{24} \int_{-1}^{1} \left(P_*^+ - P_*^-\right) \mathrm{d}y_2. \tag{30}$$

2.2. Example

Consider time-harmonic uniform loading in the form

$$P^{\pm} = A^{\pm} \left(1 - x_2^2/l_2^2\right) e^{-i\omega t} \tag{31}$$

with $A^{\pm} = const$. Time harmonic factor $e^{-i\omega t}$ is omitted below. Now, (16) gives

$$u_3^{(0)} = -\frac{A_*^+ - A_*^-}{3} \tag{32}$$

where $A_*^{\pm}$ is scaled as in (6). Also, the coefficients in complementary solution (20) become

$$A_n = -\frac{2\cos\beta_n (A_*^+ + A_*^-)}{\delta\, \beta_n^3 \sinh \beta_n \delta}, \quad B_n = -\frac{2\cos\beta_n (A_*^+ - A_*^-)}{\delta\, \beta_n^3 \cosh \beta_n \delta}. \tag{33}$$

In addition, the coefficients in the formula for the particular solution take the form

$$a_1 = \frac{A_*^+ - A_*^-}{6}, \quad a_2 = \frac{A_*^+ + A_*^-}{3}, \quad a_3 = -\frac{A_*^+ - A_*^-}{18}. \tag{34}$$

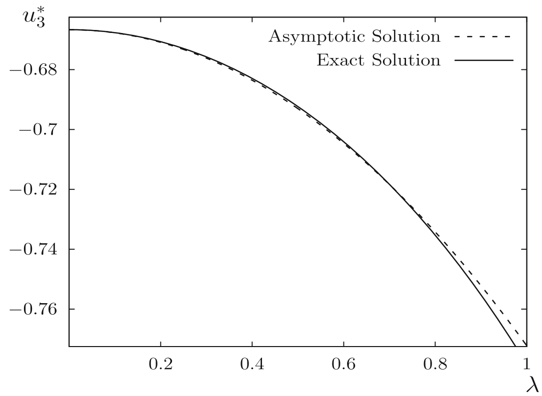

FIG. 2. Comparison of asymptotic (35) and exact (85) formulae for $u_3^*(0,0)$ at $A_*^+ = -A_*^- = 1$ and $\delta = 1$

Hence

$$u_3^* = -\frac{A_*^+ - A_*^-}{3} + \lambda^2 \left(\frac{1}{3} \left(\frac{A_*^+ - A_*^-}{2} y_1^2 + (A_*^+ + A_*^-) y_1 - \frac{A_*^+ - A_*^-}{6} \right) \right.$$
$$\left. - \frac{2}{\delta \pi^3} \sum_{n=1}^{\infty} \frac{\cos \beta_n}{n^3} \left(\frac{(A_*^+ - A_*^-) \cosh \beta_n \delta y_1}{\sinh \beta_n \delta} + \frac{(A_*^+ + A_*^-) \sinh \beta_n \delta y_1}{\cosh \beta_n \delta} \right) \times \right.$$
$$\left. \times \cos \beta_n y_2 \right) + \cdots . \tag{35}$$

It can be easily verified that the last two-term asymptotic behaviour is identical to its counterpart following from exact solution (85) presented in "Appendix".

The acceleration at the centre, in this case, takes the form

$$a = l_1 \omega^2 \left(\frac{A_*^+ - A_*^-}{3} + \lambda^2 \left(\frac{A_*^+ - A_*^-}{18} + \frac{2}{\delta \pi^3} \sum_{n=1}^{\infty} \frac{\cos \beta_n}{n^3} \frac{A_*^+ - A_*^-}{\sinh \beta_n \delta} \right) + \cdots \right) \tag{36}$$

leading to a correction to the classical rigid body dynamics expressed as

$$m\, a = F + k \frac{\partial^2 F}{\partial t^2} \tag{37}$$

whereas before $m = l_1\, l_2\, \rho$,

$$F = \frac{A^+ - A^-}{3} \tag{38}$$

and

$$k = \frac{l_1^2}{c_2^2} \left(\frac{1}{6} + \frac{6}{\delta \pi^3} \sum_{n=1}^{\infty} \frac{\cos \beta_n}{n^3 \sinh \beta_n \delta} \right). \tag{39}$$

Outside the centre, formula (35) is also valid for taking into account the effect of self-equilibrated low-frequency loading, when $A_*^+ = A_*^-$. Obviously, the classical rigid body model is not applicable in the latter case.

Below we present numerical results for $A_*^+ = -A_*^- = 1$ and $\delta = 1$. Figure 2 displays comparison of asymptotic formula (35) and exact solution (85) for the non-dimensional displacement u_3^* plotted against the frequency λ. It is seen that the asymptotic formula is efficient even for non-small values of frequency. Figure 3 displays the relative errors ε for the leading order ($u_3^* = u_3^{(0)}$) and next order ($u_3^* = u_3^{(0)} + \lambda^2 u_3^{(1)}$) approximation with respect to the exact solution.

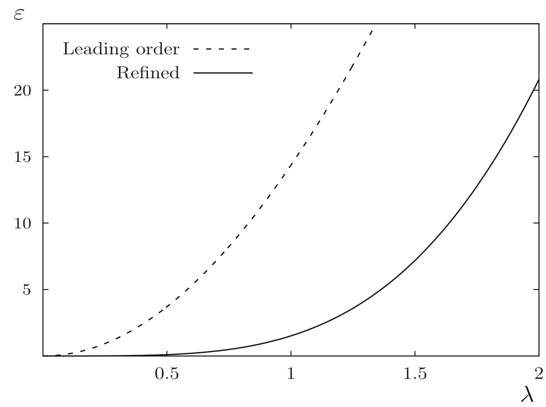

FIG. 3. Comparison of relative errors for leading order (32) and next order (35) approximation at $y_1 = y_2 = 0$ for $A_*^+ = -A_*^- = 1$ and $\delta = 1$

3. Plane problem

In this section, we investigate in-plane motion of the same elastic rectangle as in the previous section subject to longitudinal loads at $x_1 = \pm l_1$, see Fig. 1. The equations of motion and boundary conditions are written as

$$\sigma_{ij,j} = \rho u_{i,tt} \ , \quad i, j = 1, 2 \tag{40}$$

and

$$\sigma_{11}(\pm l_1, x_2, t) = P^{\pm}, \quad \sigma_{12}(\pm l_1, x_2, t) = 0, \quad \sigma_{2i}(x_1, \pm l_2, t) = 0, \quad i = 1, 2 \tag{41}$$

with

$$\begin{aligned} \sigma_{ii} &= \frac{E(1-\nu)}{(1+\nu)(1-2\nu)}\, u_{i,i} + \frac{E\nu}{(1+\nu)(1-2\nu)} u_{j,j} \\ \sigma_{ij} &= \frac{E}{2(1+\nu)}(u_{i,j} + u_{j,i}), \quad i \neq j = 1, 2 \end{aligned} \tag{42}$$

where $P^{\pm} = P^{\pm}(x_2, t)$ are again assumed to be even in x_2.

3.1. Perturbation procedure

As above, we adopt the same small parameter λ defined by (4) and use the scaling

$$y_i = \frac{x_i}{l_i}, \quad \tau = \frac{t}{T}, \quad \sigma_{ij}^* = \frac{\sigma_{ij}}{\lambda^2 \rho\, c_2^2}, \quad u_i^* = \frac{u_i}{l_1}, \quad P_*^{\pm} = \frac{P^{\pm}}{\lambda^2 \rho\, c_2^2}, \quad i, j = 1, 2, \tag{43}$$

which is similar to (5) and (6). In order to consider the low-frequency motions of the rectangle, the small parameter defined in (4) is employed. Formulae (40) and (42) can be rewritten as

$$\begin{aligned} \sigma_{11,1}^* + \delta \sigma_{12,2}^* &= u_{1,\tau\tau}^*, \\ \sigma_{12,1}^* + \delta \sigma_{22,2}^* &= u_{2,\tau\tau}^*, \end{aligned} \tag{44}$$

and

$$\begin{aligned} \lambda^2 \sigma_{11}^* &= \kappa^2\, u_{1,1}^* + \delta\, (\kappa^2 - 2)\, u_{2,2}^*, \\ \lambda^2 \sigma_{12}^* &= \delta\, u_{1,2}^* + u_{2,1}^*, \\ \lambda^2 \sigma_{22}^* &= \delta\, \kappa^2\, u_{2,2}^* + (\kappa^2 - 2)\, u_{1,1}^* \end{aligned} \tag{45}$$

where $\kappa^2 = 2(1-\nu)/(1-2\nu)$.

Let us now expand the displacement and stress components into the asymptotic series

$$\begin{aligned} u_i^* &= u_i^{(0)} + \lambda^2 u_i^{(1)} + \cdots, \\ \sigma_{ii}^* &= \sigma_{ii}^{(0)} + \lambda^2 \sigma_{ii}^{(1)} + \cdots, \\ \sigma_{ij}^* &= \sigma_{ij}^{(0)} + \lambda^2 \sigma_{ij}^{(1)} + \cdots, \quad i \neq j = 1, 2. \end{aligned} \tag{46}$$

On substituting expansions (46) into equations (44) and (45), we arrive at leading order to the boundary value problem given by

$$\begin{aligned} \sigma_{11,1}^{(0)} + \delta \sigma_{12,2}^{(0)} &= u_{1,\tau\tau}^{(0)}, \\ \sigma_{12,1}^{(0)} + \delta \sigma_{22,2}^{(0)} &= u_{2,\tau\tau}^{(0)}, \end{aligned} \tag{47}$$

with

$$\begin{aligned} &\kappa^2\, u_{1,1}^{(0)} + \delta\, (\kappa^2 - 2)\, u_{2,2}^{(0)} = 0, \\ &\delta\, u_{1,2}^{(0)} + u_{2,1}^{(0)} = 0, \\ &\delta\, \kappa^2\, u_{2,2}^{(0)} + (\kappa^2 - 2)\, u_{1,1}^{(0)} = 0, \end{aligned} \tag{48}$$

and

$$\sigma_{11}^{(0)}\Big|_{y_1=\pm 1} = P_*^{\pm}, \quad \sigma_{12}^{(0)}\Big|_{y_1=\pm 1} = 0, \qquad \sigma_{i2}^{(0)}\Big|_{y_2=\pm 1} = 0, \quad i = 1, 2. \tag{49}$$

From Eqs. (48_1) and (48_3), we obtain

$$u_{1,1}^{(0)} = u_{2,2}^{(0)} = 0, \tag{50}$$

resulting in

$$u_1^{(0)} = u_1^{(0)}(y_2, \tau), \quad u_2^{(0)} = u_2^{(0)}(y_1, \tau). \tag{51}$$

Substituting (51) into (48_2), we have

$$u_i^{(0)} = U_i(\tau), \quad i = 1, 2, \tag{52}$$

corresponding to rigid body translation of rectangle. Thus, Eqs. (47_1) and (47_2) become

$$\begin{aligned} \sigma_{11,1}^{(0)} + \delta \sigma_{12,2}^{(0)} &= U_{1,\tau\tau}, \\ \sigma_{12,1}^{(0)} + \delta \sigma_{22,2}^{(0)} &= U_{2,\tau\tau}. \end{aligned} \tag{53}$$

Integrating (53_1) over the rectangular region, we derive

$$\begin{aligned} &\int_{-1}^{1}\int_{-1}^{1} \frac{\partial \sigma_{11}^{(0)}}{\partial y_1} \mathrm{d}y_1 \mathrm{d}y_2 + \delta \int_{-1}^{1}\int_{-1}^{1} \frac{\partial \sigma_{12}^{(0)}}{\partial y_2} \mathrm{d}y_2 \mathrm{d}y_1 \\ &\quad = \int_{-1}^{1} \left(\sigma_{11}^{(0)}\Big|_{y_1=1} - \sigma_{11}^{(0)}\Big|_{y_1=-1} \right) \mathrm{d}y_2 + \delta \int_{-1}^{1} \left(\sigma_{12}^{(0)}\Big|_{y_2=1} - \sigma_{12}^{(0)}\Big|_{y_2=-1} \right) \mathrm{d}y_1 \\ &\quad = \int_{-1}^{1} \left(P_*^+ - P_*^- \right) \mathrm{d}y_2 = 4U_{1,\tau\tau}. \end{aligned} \tag{54}$$

Similarly, integrating (53_2) and applying the last boundary conditions in (49), we arrive at $U_2(\tau) = 0$. Thus,

$$u^{(0)}_{1,\tau\tau} = \frac{1}{4}\int\limits_{-1}^{1} \left(P^{+}_{*} - P^{-}_{*}\right) \mathrm{d}y_2, \tag{55}$$

which corresponds to Newton's second law, similarly to Eqs. (16) and (17).

At next order, we have a pseudo-static boundary value problem given by

$$\begin{aligned}
&\kappa^2 \frac{\partial^2 u^{(1)}_1}{\partial y_1^2} + \delta^2 \frac{\partial^2 u^{(1)}_1}{\partial y_2^2} + \delta(\kappa^2 - 1)\frac{\partial^2 u^{(1)}_2}{\partial y_1 \partial y_2} = \frac{1}{4}\int\limits_{-1}^{1} \left(P^{+}_{*} - P^{-}_{*}\right) \mathrm{d}y_2,\\
&\delta^2\kappa^2 \frac{\partial^2 u^{(1)}_2}{\partial y_2^2} + \frac{\partial^2 u^{(1)}_2}{\partial y_1^2} + \delta(\kappa^2 - 1)\frac{\partial^2 u^{(1)}_1}{\partial y_1 \partial y_2} = 0
\end{aligned} \tag{56}$$

with

$$\begin{aligned}
&\delta\, u^{(1)}_{1,2} + u^{(1)}_{2,1}\Big|_{y_2=\pm 1} = 0,\\
&\delta\, u^{(1)}_{1,2} + u^{(1)}_{2,1}\Big|_{y_1=\pm 1} = 0,\\
&\delta\, \kappa^2\, u^{(1)}_{2,2} + (\kappa^2 - 2)\, u^{(1)}_{1,1}\Big|_{y_2=\pm 1} = 0,\\
&\kappa^2\, u^{(1)}_{1,1} + \delta\, (\kappa^2 - 2)\, u^{(1)}_{2,2}\Big|_{y_1=\pm 1} = P^{\pm}_{*}.
\end{aligned} \tag{57}$$

This elliptic problem for a rectangle may be reduced to a bi-harmonic equation which received a lot of attention in numerous publication, see [19–21] and references therein. At the same time, its solution cannot be expressed in a simple explicit form.

3.2. Elongated rectangle

In what follows, we restrict our analysis to an elongated rectangle for a small parameter $\eta = \delta^{-1}$. In this case, we consider only outer expansion ignoring the inner one corresponding to localized near the edges $y_1 = \pm 1$, e.g. see [22–24]. First, we specify scaled displacements v_i, $i = 1, 2$, as

$$u^{(1)}_1 = \frac{v_1}{4}\int\limits_{-1}^{1} \left(P^{+}_{*} - P^{-}_{*}\right) \mathrm{d}y_2, \quad u^{(1)}_2 = \eta\, \frac{v_2}{4}\int\limits_{-1}^{1} \left(P^{+}_{*} - P^{-}_{*}\right) \mathrm{d}y_2. \tag{58}$$

Then, we get a boundary value problem given by

$$\begin{aligned}
&\frac{\partial^2 v_1}{\partial y_2^2} + \eta^2\left(\kappa^2 \frac{\partial^2 v_1}{\partial y_1^2} + (\kappa^2 - 1)\frac{\partial^2 v_2}{\partial y_1 \partial y_2} - 1\right) = 0,\\
&\kappa^2 \frac{\partial^2 v_2}{\partial y_2^2} + (\kappa^2 - 1)\frac{\partial^2 v_1}{\partial y_1 \partial y_2} + \eta^2 \frac{\partial^2 v_2}{\partial y_1^2} = 0
\end{aligned} \tag{59}$$

with

$$\begin{aligned}
&v_{1,2} + \eta^2 v_{2,1}\big|_{y_2=\pm 1} = 0,\\
&v_{1,2} + \eta^2 v_{2,1}\big|_{y_1=\pm 1} = 0,
\end{aligned}$$

$$
\begin{aligned}
&(\kappa^2-2)\, v_{1,1} + \kappa^2\, v_{2,2}\big|_{y_2=\pm 1} = 0, \\
&\kappa^2\, v_{1,1} + (\kappa^2-2)\, v_{2,2}\big|_{y_1=\pm 1} = \frac{4P_*^{\pm}}{\int\limits_{-1}^{1}\left(P_*^+ - P_*^-\right)\mathrm{d}y_2}.
\end{aligned}
\tag{60}
$$

We are looking for the solution of (59)–(60) in the form

$$
v_i = v_i^{(0)} + \eta^2 v_i^{(1)} + \cdots, \quad i = 1, 2. \tag{61}
$$

At leading order

$$
\frac{\partial^2 v_1^{(0)}}{\partial y_2^2} = 0, \qquad \kappa^2 \frac{\partial^2 v_2^{(0)}}{\partial y_2^2} + (\kappa^2-1)\frac{\partial^2 v_1^{(0)}}{\partial y_1 \partial y_2} = 0 \tag{62}
$$

subject to

$$
\left.\frac{\partial v_1^{(0)}}{\partial y_2}\right|_{y_2=\pm 1} = 0, \quad \left.\frac{\partial v_1^{(0)}}{\partial y_2}\right|_{y_1=\pm 1} = 0, \quad \left.(\kappa^2-2)\,\frac{\partial v_1^{(0)}}{\partial y_1} + \kappa^2\,\frac{\partial v_2^{(0)}}{\partial y_2}\right|_{y_2=\pm 1} = 0 \tag{63}
$$

and

$$
\left.\kappa^2\,\frac{\partial v_1^{(0)}}{\partial y_1} + (\kappa^2-2)\,\frac{\partial v_2^{(0)}}{\partial y_2}\right|_{y_1=\pm 1} = \frac{4P_*^{\pm}}{\int\limits_{-1}^{1}\left(P_*^+ - P_*^-\right)\mathrm{d}y_2}. \tag{64}
$$

The sought for symmetric solution of the boundary value problem (62)–(63) takes the form

$$
v_1^{(0)} = V(y_1, \tau), \quad v_2^{(0)} = -\frac{\kappa^2-2}{\kappa^2} y_2 \frac{\partial V}{\partial y_1} \tag{65}
$$

where V is an unknown function. Then, using Saint-Venant's principle [23,24], boundary conditions (64) can be written as

$$
\left.\frac{\partial V}{\partial y_1}\right|_{y_1=\pm 1} = \frac{\kappa^2}{2(\kappa^2-1)\int\limits_{-1}^{1}\left(P_*^+ - P_*^-\right)\mathrm{d}y_2} \int\limits_{-1}^{1} P_*^{\pm}\mathrm{d}y_2. \tag{66}
$$

At next order

$$
\begin{aligned}
&\frac{\partial^2 v_1^{(1)}}{\partial y_2^2} + \kappa^2 \frac{\partial^2 v_1^{(0)}}{\partial y_1^2} + (\kappa^2-1)\frac{\partial^2 v_2^{(0)}}{\partial y_1 \partial y_2} = 1, \\
&\kappa^2 \frac{\partial^2 v_2^{(1)}}{\partial y_2^2} + (\kappa^2-1)\frac{\partial^2 v_1^{(1)}}{\partial y_1 \partial y_2} + \frac{\partial^2 v_2^{(0)}}{\partial y_1^2} = 0
\end{aligned}
\tag{67}
$$

with

$$
\begin{aligned}
&\left.\frac{\partial v_1^{(1)}}{\partial y_2} + \frac{\partial v_2^{(0)}}{\partial y_1}\right|_{y_2=\pm 1} = 0, \\
&\left.\frac{\partial v_1^{(1)}}{\partial y_2} + \frac{\partial v_2^{(0)}}{\partial y_1}\right|_{y_1=\pm 1} = 0, \\
&\left.(\kappa^2-2)\,\frac{\partial v_1^{(1)}}{\partial y_1} + \kappa^2\,\frac{\partial v_2^{(1)}}{\partial y_2}\right|_{y_2=\pm 1} = 0
\end{aligned}
\tag{68}
$$

and

$$
\left.\kappa^2\,\frac{\partial v_1^{(1)}}{\partial y_1} + (\kappa^2-2)\,\frac{\partial v_2^{(1)}}{\partial y_2}\right|_{y_1=\pm 1} = 0. \tag{69}
$$

On substituting formulae (65) into Eq. (67_1) and boundary condition (68_1), we obtain

$$\frac{\partial^2 V}{\partial y_1^2} = \frac{\kappa^2}{4(\kappa^2-1)}. \tag{70}$$

Its solution is

$$V(y_1,\tau) = \frac{\kappa^2 y_1^2}{8(\kappa^2-1)} + b_1 y_1 + b_2 \tag{71}$$

with

$$b_1 = \frac{\kappa^2}{4(\kappa^2-1)\int\limits_{-1}^{1}\left(P_*^+ - P_*^-\right)\mathrm{d}y_2}\int\limits_{-1}^{1}\left(P_*^+ + P_*^-\right)\mathrm{d}y_2, \tag{72}$$

see (66).

In order to determine the coefficient, b_2, we proceed with a higher-order approximation for stresses. Starting from (44) and (58), we have

$$\sigma_{11,1}^{(1)} + \frac{1}{\eta}\sigma_{12,2}^{(1)} = u_{1,\tau\tau}^{(1)} \tag{73}$$

with

$$\left.\sigma_{12}^{(1)}\right|_{y_2=\pm 1} = 0. \tag{74}$$

In the above, $u_1^{(1)}$ may be expressed in terms of V according to (58) and (65). Integrating Eq. (73) over the rectangular region and using boundary condition (74) together with

$$\int\limits_{-1}^{1}\sigma_{11}^{(1)}\mathrm{d}y_1 = 0 \tag{75}$$

coming from Saint-Venant's principle finally result in

$$\left.\left(\frac{\kappa^2\ y_1^2}{24(\kappa^2-1)} + b_2\ y_1\right)\right|_0^1 \frac{\partial^2}{\partial\tau^2}\int\limits_{-1}^{1}\left(P_*^+ - P_*^-\right)\mathrm{d}y_2 = 0. \tag{76}$$

Thus,

$$b_2 = -\frac{\kappa^2}{24(\kappa^2-1)}. \tag{77}$$

3.3. 1D problem for plate extension

The problem in this section can be also considered within the framework of 1D theory for plate extension [22]. The related equation of motion and boundary condition are written as

$$\frac{E}{1-\nu^2}\frac{d^2u}{dx_1^2} + \rho\,\omega^2 u = 0 \tag{78}$$

and

$$\left.\frac{2\,E\,l_1}{1-\nu^2}\frac{du}{dx_1}\right|_{x_1=\pm l_1} = \int\limits_{-l_1}^{l_1} A^{\pm}\mathrm{d}x_2. \tag{79}$$

In the expression for stress resultant $A^{\pm} = P^{\pm}e^{i\omega t}$, the exponential factor is omitted.

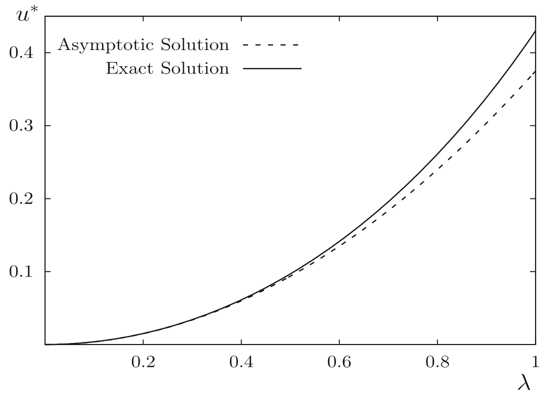

Fig. 4. Comparison of asymptotic (84) and (88) displacements at $y_1 = 1$, $A_*^+ = A_*^- = 1$ and $\nu = 0.25$

Specifying the scaled quantities

$$\sigma_{11}^* = \frac{\sigma_{11}}{\lambda^2 \rho\, c_2^2}, \quad u^* = \frac{u}{l_1}, \quad A_*^\pm = \frac{A^\pm}{\lambda^2 \rho\, c_2^2} \tag{80}$$

and asymptotic expansions

$$\begin{aligned} u^* &= u^{(0)} + \lambda^2 u^{(1)} + \cdots, \\ \sigma_{11}^* &= \sigma_{11}^{(0)} + \lambda^2 \sigma_{11}^{(1)} + \cdots, \end{aligned} \tag{81}$$

the solution of problem (78) with (79) can be obtained in a very similar manner as above. It is given by

$$u^{(0)} = -\frac{1}{4}\int_{-1}^{1} \left(A_*^+ - A_*^-\right) \mathrm{d}y_2, \tag{82}$$

and

$$u^{(1)} = \frac{1-\nu}{4}\left(u^{(0)}\, y_1^2 + \frac{y_1}{2}\int_{-1}^{1}\left(A_*^+ + A_*^-\right)\mathrm{d}y_2 + \frac{u^{(0)}}{3}\right), \tag{83}$$

where all the coefficients can be obtained from (71), (72) and (77). Therefore, expansion (81) for longitudinal displacement u coincides with the earlier derived approximation for u_1.

For uniform loading ($A_*^\pm = \text{const}$), we have from (80) and (83)

$$u^* = -\frac{1}{2}(A_*^+ - A_*^-) + \lambda^2 \frac{\gamma^2}{2}\left(\frac{A_*^+ - A_*^-}{2} y_1^2 + (A_*^+ + A_*^-) y_1 - \frac{A_*^+ - A_*^-}{6}\right) + \cdots. \tag{84}$$

Numerical comparisons with the full solution of the studied 1D problem, see "Appendix", are presented in Figs. 4 and 5 for $\nu = 0.25$ at $y_1 = 1$. Both self-equilibrated ($A_*^+ = A_*^- = 1$) and non-self-equilibrated ($A_*^+ = -A_*^- = 1$) types of loading are analysed.

4. Conclusions

The first-order low-frequency corrections to rigid body translations of an elastic rectangle are derived for a class of prescribed stresses applied to its two opposite sides. They take into consideration the deformations of the rectangle and allow calculating the variation of stresses and displacements over its

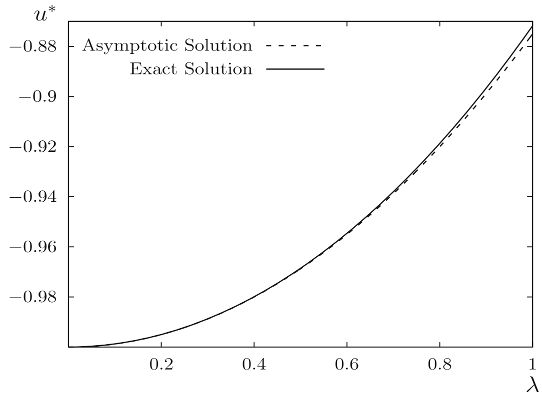

Fig. 5. Comparison of asymptotic (84) and (88) displacements at $y_1 = 1$, $A_*^+ = -A_*^- = 1$ and $\nu = 0.25$

interior, including the case of a self-equilibrated loading, which cannot be treated within the classical rigid body model.

The obtained corrections are determined by solving inhomogeneous pseudo-static problems for a rectangle, for which inertial terms in the equations of motions are omitted. For the anti-plane problem, the correction takes an explicit form, e.g. see refined formula (37), in which the coefficient at $\partial^2 F/\partial t^2$ is expressed through the rapidly convergent series (39). For the plane problem, explicit results are only available for an elongated rectangle, which may be also analysed using the elementary theory for plate extension, see Sect. 3.2. Although the static plane problem has no closed formed in the general set-up, it can be reduced to the well-known bi-harmonic problem, e.g. see [19–21].

The developed perturbation techniques may be easily extended to an arbitrary set of stresses applied to the sides of a rectangle, including the stresses resulting not only in rigid body translations but also in rigid body rotations. For an elongated rectangle, corrections to in-plane rotations may be also deduced from the Kirchhoff theory for plate bending, similarly to [11], which also considers the effects of inhomogeneity and viscosity. Finally, the developed methodology seems to have a potential to be implemented for three-dimensional solids and more general geometries.

5. Appendix

5.1. Anti-plane problem for rectangle

Time-dependent dimensionless solution of problem (1)–(3) at $Q^\pm = 0$ and $P^\pm$ given by (31) is written as

$$u_3^*(y_1, y_2) = C_0 \cos\lambda\, y_1 + D_0 \sin\lambda\, y_1 + \sum_{n=1}^{\infty} (C_n \cosh\alpha_n\, y_1 + D_n \sinh\alpha_n\, y_1)\cos\beta_n\, y_2 \tag{85}$$

where

$$C_0 = -\frac{2(1+\nu)(A^+ - A^-)}{3\lambda\, E\, \sin\lambda}, \quad D_0 = \frac{2(1+\nu)(A^+ + A^-)}{3\lambda\, E\, \cos\lambda}, \tag{86}$$

and

$$C_n = -\frac{4(1+\nu)\cos\beta_n\,(A^+ - A^-)}{E\,\alpha_n\,\beta_n^2\,\sinh\alpha_n}, \quad D_n = -\frac{4(1+\nu)\cos\beta_n\,(A^+ + A^-)}{E\alpha_n\,\beta_n^2\,\cosh\alpha_n}, \quad n = 1, 2, 3\ldots \tag{87}$$

with $\alpha_n = \sqrt{\delta^2\beta_n^2 - \lambda^2}$ and $\beta_n = n\,\pi$. In the above $u_3^* = u_3/l_1$ and $y_i = x_i/l_i$, $i = 1, 2$.

5.2. Plate extension

The solution of problem (78) and (79) is given by

$$u^* = C\cos\gamma\lambda y_1 + D\sin\gamma\lambda y_1 \tag{88}$$

where

$$C = -\frac{\gamma\ \lambda}{4\ \sin\gamma\ \lambda}\int_{-1}^{1}\left(A_*^+ - A_*^-\right)\mathrm{d}y_2, \qquad D = \frac{\gamma\ \lambda}{4\ \cos\gamma\ \lambda}\int_{-1}^{1}\left(A_*^+ + A_*^-\right)\mathrm{d}y_2. \tag{89}$$

with $u_3^* = u_3/l_1$ and $y_1 = x_1/l_1$.

Publisher's Note Springer Nature remains neutral with regard to jurisdictional claims in published maps and institutional affiliations.

References

[1] Rao, A.: Dynamics of Particles and Rigid Bodies: A Systematic Approach. Cambridge University Press, Cambridge (2006)
[2] Milton, G.W., Willis, J.R.: On modifications of Newton's second law and linear continuum elastodynamics. Proc. R. Soc. A Math. Phys. Eng. Sci. **463**(2079), 855–880 (2007)
[3] Huang, H.H., Sun, C.T., Huang, G.L.: On the negative effective mass density in acoustic metamaterials. Int. J. Eng. Sci. **47**(4), 610–617 (2009)
[4] Lee, S.H., Park, C.M., Seo, Y.M., Wang, Z.G., Kim, C.K.: Acoustic metamaterial with negative density. Phys. Lett. A **373**(48), 4464–4469 (2009)
[5] Yao, S., Zhou, X., Hu, G.: Experimental study on negative effective mass in a 1D mass-spring system. New J. Phys. **10**(4), 043020 (2008)
[6] Wang, X.: Dynamic behaviour of a metamaterial system with negative mass and modulus. Int. J. Solids Struct. **51**(7–8), 1534–1541 (2014)
[7] Mei, J., Liu, Z., Wen, W., Sheng, P.: Effective dynamic mass density of composites. Phys. Rev. B **76**(13), 134205 (2007)
[8] Shestakova, A.: Development of mathematical models for freight cars subject to dynamic loading. PhD Thesis, Keele University (2015)
[9] Ansari, M., Esmailzadeh, E., Younesian, D.: Longitudinal dynamics of freight trains. Int. J. Heavy Veh. Syst. **16**(1–2), 102–131 (2009)
[10] Wu, Q., Spiryagin, M., Cole, C.: Longitudinal train dynamics: an overview. Veh. Syst. Dyn. **54**(12), 1688–1714 (2016). ISO 690
[11] Kaplunov, J., Shestakova, A., Aleynikov, I., Hopkins, B., Talonov, A.: Low-frequency perturbations of rigid body motions of a viscoelastic inhomogeneous bar. Mech. Time Depend. Mater. **19**(2), 135–151 (2015)
[12] Kaplunov, J., Prikazchikov, D., Sergushova, O.: Multi-parametric analysis of the lowest natural frequencies of strongly inhomogeneous elastic rods. J. Sound Vib. **366**, 264–276 (2016)
[13] Kaplunov, J., Prikazchikov, D.A., Prikazchikova, L.A., Sergushova, O.: The lowest vibration spectra of multi-component structures with contrast material properties. J. Sound Vib. **445**, 132–147 (2019)
[14] Şahin, O.: The effect of boundary conditions on the lowest vibration modes of strongly inhomogeneous beams. J. Mech. Mater. Struct. **14**(4), 569–585 (2019)
[15] Şahin, O., Erbaş, B., Kaplunov, J., Savšek, T.: The lowest vibration modes of an elastic beam composed of alternating stiff and soft components. Arch. Appl. Mech. **90**(2), 339–352 (2020)
[16] Kurfess, T.R. (ed.): Robotics and Automation Handbook. CRC Press, Boca Raton (2018)
[17] Davim, J.P. (ed.): Introduction to Mechanical Engineering. Springer, Berlin (2018)
[18] Aleksandrov, E.V., Sokolinskii, V.B.: Applied Theory and Calculation of Impact Systems. Nauka, Moscow (1969)
[19] Meleshko, V.V.: Selected topics in the history of the two-dimensional biharmonic problem. Appl. Mech. Rev. **56**(1), 33–85 (2003)
[20] Meleshko, V.V., Gomilko, A.M.: Infinite systems for a biharmonic problem in a rectangle: further discussion. Proc. R. Soc. Lond. Ser. A Math. Phys. Eng. Sci. **460**(2043), 807–819 (2004)
[21] Kovalenko, M.D., Menshova, I.V., Kerzhaev, A.P.: On the exact solutions of the biharmonic problem of the theory of elasticity in a half-strip. Z. Angew. Math. Phys. **69**(5), 121 (2018)
[22] Kaplunov, J.D., Kossovitch, L.Y., Nolde, E.V.: Dynamics of Thin Walled Elastic Bodies. Academic Press, Cambridge (1998)

[23] Gregory, R.D., Wan, F.Y.: Decaying states of plane strain in a semi-infinite strip and boundary conditions for plate theory. J. Elast. **14**(1), 27–64 (1984)
[24] Babenkova, E., Kaplunov, J.: Low-frequency decay conditions for a semi-infinite elastic strip. Proc. R. Soc. Lond. Ser. A Math. Phys. Eng. Sci. **460**(2048), 2153–2169 (2004)

Julius Kaplunov
Department of Mathematics
Keele University
Staffordshire ST5 5BG
UK
e-mail: j.kaplunov@keele.ac.uk

Julius Kaplunov
Al-Farabi Kazakh National University
050040 Almaty
Kazakhstan

Onur Şahin
Department of Mathematics
Giresun University
Giresun
Turkey
e-mail: onur.sahin@giresun.edu.tr

(Received: May 8, 2020; revised: August 21, 2020)